Lithium–Sulfur Batteries

International Edition: DOI: 10.1002/anie.201605931
German Edition: DOI: 10.1002/ange.201605931

Enhanced Performance of a Lithium–Sulfur Battery Using a Carbonate-Based Electrolyte

Zhixin Xu, Jiulin Wang, Jun Yang, Xiaowei Miao, Renjie Chen, Ji Qian, and Rongrong Miao*

Abstract: *The lithium–sulfur battery is regarded as one of the most promising candidates for lithium–metal batteries with high energy density. However, dendrite Li formation and low cycle efficiency of the Li anode as well as unstable sulfur based cathode still hinder its practical application. Herein a novel electrolyte (1*M *LiODFB/EC-DMC-FEC) is designed not only to address the above problems of Li anode but also to match sulfur cathode perfectly, leading to extraordinary electrochemical performances. Using this electrolyte, lithium | lithium cells can cycle stably for above 2000 hours and the average Coulumbic efficiency reaches 98.8 %. Moreover, the Li–S battery delivers a reversible capacity of about 1400 mAh* g^{-1}_{sulfur} *with retention of 89 % for 1100 cycles at 1 C, and a capacity above 1100 mAh* g^{-1}_{sulfur} *at 10 C. The more advantages of this cell system are its outstanding cycle stability at 60 °C and no self-discharge phenomena.*

Nowadays, Li-ion batteries, which typically consist of graphite anode and lithium transition-metal oxide cathode, have been widely used for various electric portable devices, even for the (hybrid) electric vehicles (EVs).[1] However, the energy density of state-of-the-art Li-ion batteries is not high enough for grid-scale energy storage, space application and future all-electric vehicles competitive with petrol ones.[2] Accordingly, various "beyond Li-ion batteries" with high energy densities are being intensively explored, of which Li–S batteries are in the more advanced development state towards practical application.[3] Nonetheless, several technical challenges still limit their commercialization. Among these, the instability of Li anode has become a dominant factor limiting the cycle life and safety of Li–S batteries. How to suppress the lithium dendrite formation and improve the Coulombic efficiency during cycling are the main challenges facing Li anode.

Many different strategies have been reported to stabilize Li metal anode in Li–S batteries,[4] one possible strategy, which focuses on the electrolyte modification[5] by changing Li salts, solvents[6] or additives,[7] appears to be effective. A great progress has been achieved by using ether-based electrolytes for Li–S batteries.[8] However, the frequently used DOL-DME electrolytes suffer from low boiling and flash points, and pose significant safety risks for operation at elevated temperatures. Even more, the commonly used $LiNO_3$ additive is an oxidizing agent and provides further safety concerns.[9] In addition, the polysulfides are soluble easily in ether-based electrolytes which could result in severe shuttle effect and self-discharge for elemental sulfur based battery systems.[9] On the other hand, carbonate solvents with relatively lower vapor pressure are widely used in commercial Li-ion batteries with good performances.[9] Unfortunately, they are chemically incompatible with most sulfur cathodes,[10] except pyrolyzed polyacrylonitrile sulfur composite (S@pPAN) and the confined S_{2-4} in microporous carbon matrix.[11] Despite of the good compatibility with carbonate electrolytes, the S@pPAN based cells have not achieved the long-term cycle stability. An important reason is that conventional carbonate electrolytes containing $LiPF_6$ or LiTFSI salt could not provide a good protection of the Li anode and dendrite-free Li deposition, resulting in a low Li cycle efficiency and fast electrolyte decomposition.[12]

As mentioned above, the cycle stability and reliability of Li–S batteries involves multi-factors, such as Li deposition morphology, Coulombic efficiencies on both anode and cathode, interfacial property, thermal stability, self-discharge and others. So far, most of the approaches only pay an attention on part of them. Therefore, it is highly desirable to find effective electrolytes or other technical approaches to address all these issues and radically promote the electrochemical performance of the Li–S battery system for practical application. In view of the good thermal and hydrolytic stability as well as outstanding filming capability, lithium oxalyldifluoroborate (LiODFB) salt has been tested as an electrolyte component for Li-ion and Li–S cells.[13] More or less, a positive effect was achieved. Here we propose a new carbonate-based electrolyte system of 1M LiODFB in EC-DMC-FEC (4.5:4.5:1 v/v/v) carbonate solvents (abbr. as LiODFB/EC-DMC-FEC) for Li–S@pPAN batteries. The formulas of all the electrolyte components and characterization of LiODFB are exhibited in Figure S1 (see the Supporting Information). It has high ionic conductivity (7.2 mS cm^{-1}) at room temperature and a wide electrochemical window (> 5.5 V vs. Li/Li^+, Figure 1 a). More importantly, it demonstrates excellent compatibility with both Li anode and sulfur composite cathode.

Cu | Li cells were assembled to examine lithium deposition/dissolution cycle efficiency and stability in different electrolytes. It can be observed from Figure 1 b that the first Columbic efficiency reaches to 90.6 % in LiODFB/EC-DMC-

[*] Z. X. Xu, Prof. J. L. Wang, Prof. J. Yang, X. W. Miao, R. R. Miao
Shanghai Electrochemical Energy Devices Research Center, School of Chemistry and Chemical Engineering, Shanghai Jiao Tong University
Shanghai 200240 (China)
E-mail: yangj723@sjtu.edu.cn
Prof. R. J. Chen, J. Qian
School of Material Science & Engineering, Beijing Institute of Technology
Beijing 100081 (China)
Supporting information and the ORCID identification number(s) for the author(s) of this article can be found under http://dx.doi.org/10.1002/anie.201605931.

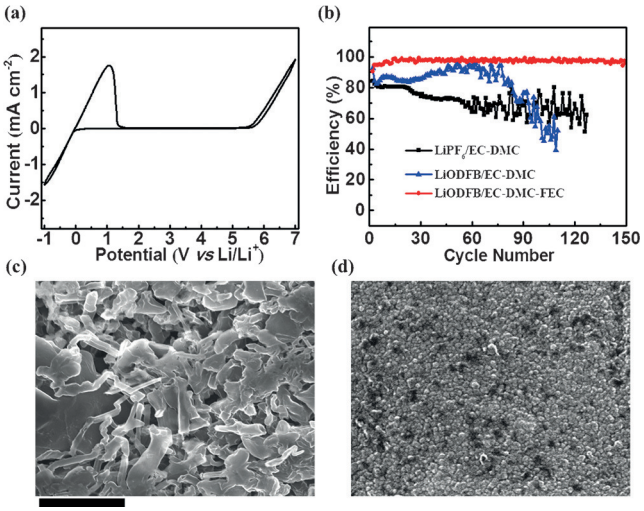

Figure 1. a) Cyclic voltammogram of Pt disc electrode in LiODFB/EC-DMC-FEC at a scanning rate of 10 mV s^{-1}. b) Coulombic efficiency vs. cycle number for different electrolyte solutions. c,d) Images of Li electrodes in Li | Li cells with 0.28 mA cm^{-2} after 100 cycles using LiPF$_6$/EC-DMC and LiODFB/EC-DMC-FEC electrolytes, respectively. Scale bar = 10 μm.

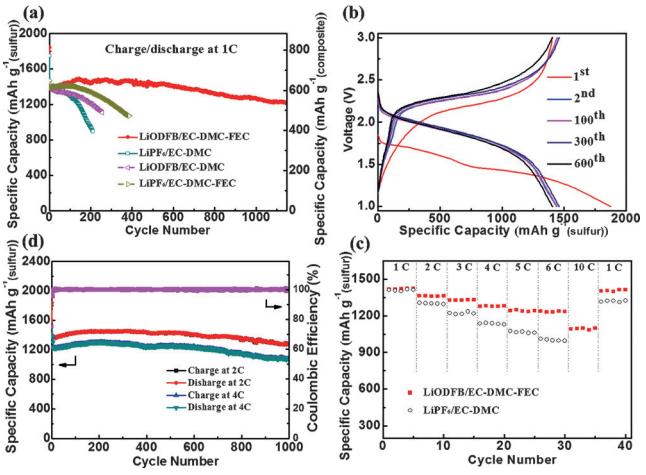

Figure 2. Electrochemical performance of Li–S batteries in different electrolytes. a) Long-term cycling performance at 25 °C. b) Charge/discharge profiles at 1 C in LiODFB/EC-DMC-FEC. c) Rate performance. d) Charge/discharge capacity and Coulombic efficiency at 2 C and 4 C in LiODFB/EC-DMC-FEC.

FEC and after several cycles it becomes stable, approximating 98 %, which is much higher than those in the FEC-free electrolytes. Considering the practical partial Li utilization, the average Coulumbic efficiency of about 98.8 % is obtained according to Figure S2 which was further measured and calculated by an equation proposed previously.[14]

A Li | Li cell was further cycled to investigate the voltage polarization and interfacial stability of the Li metal anode in LiODFB/EC-DMC-FEC. Some voltage fluctuation up to 50 mV at the primary cycling stage can be observed in Figure S3 a, which could be due to the surface morphology evolution and the establishment of a SEI film. Then, the polarization declines gradually and reaches to the stable state with a low polarization voltage (ca. 20 mV) for over 2000 h (i.e. 666 cycles) at a current density of 0.28 mA cm^{-2}. However, use of the LiPF$_6$/EC-DMC electrolyte resulted in erratic voltage response and higher voltage polarization as shown in Figure S3 b. On the other hand, it should be mentioned that FEC component is indispensable in the LiODFB/EC-DMC-FEC electrolyte system for achieving the excellent electrochemical performance. Without it, not only is the Li cycle efficiency low (Figure 1 b), but also Li | Li cell presents unstable and higher voltage polarization (Figure S3 c). A further test shows that higher FEC content than 10 % cannot enhance the Li cycle efficiency but reduce the ionic conductivity of the electrolyte. The surface morphologies of Li electrodes cycled in two solutions are shown in Figure 1 c and 1 d. The lithium deposit in LiPF$_6$/EC-DMC electrolyte is dendritic and spongy. In contrast, it is even and compact with fine spherical particles when using the proposed electrolyte (Figure 1 d).

The effect of the electrolyte composition on the cycle performance of Li–S batteries is further evaluated. All the S@pPAN samples contain 44.1 % S except mentioned else. Specific capacity was calculated based on the mass of sulfur and the capacity retention was calculated against the 2nd cycle. Figure 2 a shows the cycle behavior of Li–S batteries with different electrolytes. The capacity gradually decays in the LiPF$_6$/EC-DMC electrolyte before 100 cycles and then drops rapidly with only 66 % capacity retention after 200 cycles. The replacement of LiPF$_6$ by LiODFB can improve the cycle performance distinctly. Furthermore, it is noted that addition of FEC to the above electrolytes can effectively prolong the cycle life. Particularly, by use of LiODFB/EC-DMC-FEC the capacity retention of the cathode reaches 89 % after 1100 cycles, which corresponds to an inappreciable capacity decay of 0.01 % per cycle. Almost overlapped discharge profiles from 2nd to 600th cycle in Figure 2 b indicate the high electrochemical reversibility. After several initial cycles, the cathode capacity reaches more than 1410 mAh g$^{-1}_{sulfur}$ (i.e. 622 mAh g$^{-1}_{composite}$) at 1 C (= 1,672 mA g^{-1}), indicating a sulfur utilization approaching 85 %.

Moreover, the cells using the proposed electrolyte can deliver high power for charge/discharge cycling. As shown in Figure 2 c, with increasing the current rate from 1 C to 6 C, about 90 % of the discharge capacity can be held in LiODFB/EC-DMC-FEC. Even at extremely high rate of 10 C, the capacity is maintained at about 1100 mAh g$^{-1}_{sulfur}$. After the rate is decreased to 1 C from 6 C, 92 % of the initial capacity is recovered for the LiPF$_6$/EC-DMC electrolyte, whereas no capacity decay is observed for the LiODFB/EC-DMC-FEC even after undergoing an impact of 10 C. Figure 2 d further demonstrates the durable high rate cyclability of the Li–S battery for 1000 cycles at 2 C and at 4 C with capacity retentions of 93 % and 88 %, respectively. The Coulombic efficiency of the cathode approaches 100 % during cycling except the first cycle. When LiPF$_6$/EC-DMC electrolyte is used, Li–S battery delivers only about 1,000 mAh g$^{-1}_{sulfur}$ at 6 C, much lower than that in LiODFB/EC-DMC-FEC. In addition, the former shows significantly stronger voltage polarization at high current rate (Figure S4).

The additional advantages of the Li–S battery using the proposed electrolyte are its excellent cycling stability at elevated temperature and negligible self-discharge. 79% of the 2nd cycle capacity is retained after 1000 cycles at 60°C (Figure S5). However, the capacity fades rapidly in $LiPF_6$/EC-DMC and only 62% capacity remains after 150 cycles, which might be attributed to the poor thermal stability of $LiPF_6$ salt and unstable interfacial property on lithium anode.[15] In addition, the overlapped discharge profiles before and after 20 days storage in Figure S6 indicate that this cell system has negligible self-discharge phenomena. Also for a half discharged cell, no capacity loss was found after 20 days storage.

The high-performance rechargeable batteries require highly reversible reactions and fast kinetics simultaneously on both electrodes. First, the LiODFB/EC-DMC-FEC electrolyte ensures the reversible Li plating and striping reactions with dendrite-free morphology as mentioned above. Its high compatibility with Li anode can be ascribed to the formation of an effective SEI layer on the Li electrode surface, which prevents a further electrolyte decomposition and lithium corrosion. XPS analysis (Figure 3a) on the cycled Li electrode

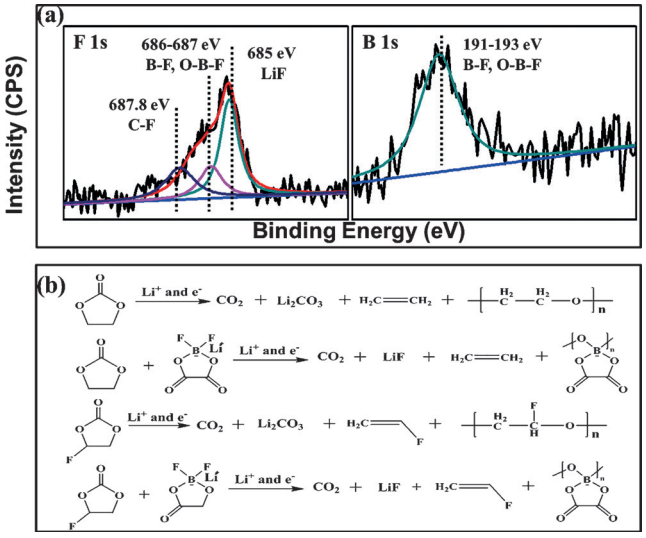

Figure 3. a) XPS spectra for F 1s and B 1s of Li electrodes in Li|Li cells with 0.28 mA cm^{-2} after 70 cycles using LiODFB/EC-DMC-FEC electrolyte. b) The proposed formation mechanism of the protective film on Li electrode in Li|Li symmetric cells.

surface reveals the species formed by the reductive decomposition and other exchanging reactions of Li salt and carbonates, but the mechanism is still unclear. We thus performed ab initio simulations in the form of the density functional theory (DFT) to deduce the reaction pathways. The proposed reactions mechanism is shown in Figure 3b and Figure S7. Li_2CO_3, LiF and short chain organic compounds arising from carbonates decomposition and their reactions with LiODFB belong to the rigid components, and carbonates decompose to form the flexible elastomers. These components are integrated to a compact and stable surface protection film, which could better accommodate the volume changes during the cycling process and prevent the side-reactions. In addition, it was reported that the formed LiF benefits the uniform and compact lithium deposits.[16] On the other hand, the main detectable decomposition products of $LiPF_6$/EC-DMC electrolyte on Li electrode are Li alkyl carbonates and alcoholic salts which can lead to a nonuniform current density distribution and lithium dendrite formation.[17] Moreover, the reiterative repair of the SEI film makes it thicker with black color, resulting in the larger interfacial resistance (Figure 4a) and higher over-potential (Figure S3b).

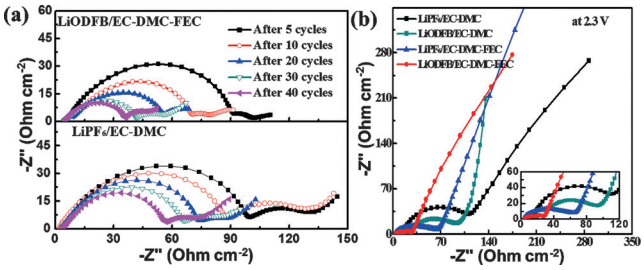

Figure 4. EIS results for Li|Li cells and Li–S batteries contained with different electrolytes. a) Li|Li cells after 5, 10, 20, 30, 40 cycles, respectively. b) Li–S batteries at the charged state after 20 cycles.

Another important reason for the long cycle life of this Li–S battery is the advanced cathode material and perfect coordination between the cathode and the electrolyte. The S@pPAN composite cathode avoids dissolution of polysulfides and the resulting shuttle reaction,[18] which often occurs for the elemental sulfur based cathodes. More interesting is that the LiODFB/EC-DMC-FEC electrolyte probably also participates in the interfacial filming reactions on the S@pPAN composite cathode, which can further improve the interfacial stability. Such a cathodic filming reaction can be inferred by the slightly lower efficiency at the 1st cycle in Figure S8. More concrete evidence is the XPS analysis as illustrated in Figure S9 . All the detectable components, including LiF, B-F species and minor high-valent sulfur species, may be favorable for the formation of a compact and thin SEI layer on both the electrodes. These surface modifications not only suppress the side-reactions, but also improve the electrode kinetics. As exhibited in Figure 4b, the Li–S battery containing LiODFB/EC-DMC-FEC presents remarkably lower interfacial resistance than those containing other electrolytes. The high electrolyte conductivity and low electrochemical resistance lead to the excellent high rate capability of the proposed battery system.

In summary, we reported a high performance Li–S battery using LiODFB/EC-DMC-FEC electrolyte. Under the synergistic effect of LiODFB and FEC, a unique SEI layer is formed on lithium anode to prevent its side-reaction with electrolyte, leading to a high Coulombic efficiency and cycle stability for lithium deposition/dissolution. Furthermore, lithium dendrites are successfully suppressed in this electrolyte during the charging process for the enhanced safety. Owing to its high ionic conductivity, high thermal stability, and very good compatibility with both Li anode and S@pPAN composite cathode, use of this electrolyte system for Li–S

battery results in extraordinary electrochemical performances, including a capacity retention of 89% for 1100 cycles, superior rate performance up to 10C, high cycle stability at 60°C and negligible self-discharge. Although the proposed electrolyte is not fit for the conventional elemental sulfur based cathodes, a higher sulfur content up to 54.8% is feasible for S@pPAN (Figure S10), which corresponds to a capacity of near 800 $mAh\,g^{-1}_{composite}$. The capacity enhancement will be our next work. We hope that the new electrolyte design concept and exceptional results presented here will greatly promote the development and practical application of high power and high energy lithium metal rechargeable batteries, especially Li–S batteries.

Experimental Section

Materials and cathode preparation. LiODFB was synthesized as described previously[19] and further purified through extraction and recrystallization using ethyl acetate/methylbenzene mixed solvents, and dried under vacuum at 70°C. Cathode preparations: PAN was mixed homogeneously with sulfur and heated at 300°C in a N_2 atmosphere. By controlling heating time S@pPAN composites with different sulfur contents, as determined by elemental analysis, were obtained. The cathode was fabricated by mixing 80 wt. % S@pPAN composite, 10 wt. % Super P and 10 wt. % carbonyl-β-cyclodextrin as a binder as reported previously,[20] then coating the mixture onto a piece of carbon-coated Al foil current collector. The electrode films were dried at 65°C in vacuum, punched in diameter of 1.2 cm and finally pressed by a pressure of 3 MPa. The electrode weight loads are about 1.5–2 $mg\,cm^{-2}$.

See the Supporting information for computation and characterizations of electrochemistry, XPS, SEM, and others.

Acknowledgements

This work was supported by the National Natural Science Foundation of China (grant number 21273146) and National Key Basic Research Program of China (grant number 2014CB932303).

Keywords: batteries · electrolytes · electrochemistry · energy storage · sulfur

How to cite: *Angew. Chem. Int. Ed.* **2016**, *55*, 10372–10375
Angew. Chem. **2016**, *128*, 10528–10531

[1] a) B. Scrosati, J. Garche, *J. Power Sources* **2010**, *195*, 2419–2430; b) J. B. Goodenough, K.-S. Park, *J. Am. Chem. Soc.* **2013**, *135*, 1167–1176; c) K. Amine, R. Kanno, Y. Tzeng, *MRS Bull.* **2014**, *39*, 395–401.
[2] G. Pistoia, Elsevier, **2014**.
[3] a) J. Hassoun, B. Scrosati, *Angew. Chem. Int. Ed.* **2010**, *49*, 2371–2374; *Angew. Chem.* **2010**, *122*, 2421–2424; b) X. Ji, K. T. Lee, L. F. Nazar, *Nat. Mater.* **2009**, *8*, 500–506; c) N. Jayaprakash, J. Shen, S. S. Moganty, A. Corona, L. A. Archer, *Angew. Chem. Int. Ed.* **2011**, *50*, 5904–5908; *Angew. Chem.* **2011**, *123*, 6026–6030.
[4] a) G. Ma, Z. Wen, J. Jin, M. Wu, X. Wu, J. Zhang, *J. Power Sources* **2014**, *267*, 542–546; b) S. J. Oh, J. K. Lee, W. Y. Yoon, *ChemSusChem* **2014**, *7*, 2562–2566; c) Z. Liu, X.-H. Zhang, C. S. Lee, *J. Mater. Chem. A* **2014**, *2*, 5602–5605.
[5] a) J. Scheers, S. Fantini, P. Johansson, *J. Power Sources* **2014**, *255*, 204–218; b) A. Manthiram, Y. Fu, S. H. Chung, C. Zu, Y. S. Su, *Chem. Rev.* **2014**, *114*, 11751–11787.
[6] L. Suo, Y. S. Hu, H. Li, M. Armand, L. Chen, *Nat. Commun.* **2013**, *4*, 1481.
[7] a) S. S. Zhang, *Electrochim. Acta* **2012**, *70*, 344–348; b) X. Liang, Z. Wen, Y. Liu, M. Wu, J. Jin, H. Zhang, *J. Power Sources* **2011**, *196*, 9839–9843; c) F. Ding, W. Xu, G. L. Graff, J. Zhang, M. L. Sushko, X. Chen, et al., *J. Am. Chem. Soc.* **2013**, *135*, 4450–4456.
[8] J. Qian, W. A. Henderson, W. Xu, P. Bhattacharya, M. Engelhard, O. Borodin, J. Zhang, *Nat. Commun.* **2015**, *6*, 6362.
[9] a) D. Aurbach, E. Pollak, R. Elazari, G. Salitra, C. S. Kelley, J. Affinito, *J. Electrochem. Soc.* **2009**, *156*, A694–A702; b) S. Zhang, K. Ueno, K. Dokko, M. Watanabe, *Adv. Energy Mater.* **2015**, *5*, 1500117; c) X. Li, A. Lushington, Q. Sun, W. Xiao, J. Liu, *Nano Lett.* **2016**, *16*, 3545–3549.
[10] a) J. Gao, M. A. Lowe, Y. Kiya, H. D. Abruna, *J. Phys. Chem. C* **2011**, *115*, 25132–25137; b) T. Yim, M. Parka, J. Yu, K. Kim, K. Im, J. Kim, et al., *Electrochim. Acta* **2013**, *107*, 454–460.
[11] a) J. Wang, J. Yang, J. Xie, N. Xu, *Adv. Mater.* **2002**, *14*, 963–965; b) J. Wang, J. Yang, C. Wang, K. Du, J. Xie, N. Xu, *Adv. Funct. Mater.* **2003**, *13*, 487–492; c) S. Xin, L. Gu, N. Zhao, Y. Yin, L. Zhou, Y. Guo, L. Wan, *J. Am. Chem. Soc.* **2012**, *134*, 18510–18513.
[12] R. Miao, J. Yang, X. Feng, H. Jia, J. Wang, Y. Nuli, *J. Power Sources* **2014**, *271*, 291–297.
[13] a) S. Zhang, *ECS Trans.* **2007**, *3*, 59–68; b) Z. Chen, Y. Qin, J. Liu, K. Amine, *Electrochem. Solid-State Lett.* **2009**, *12*, A69–A72; c) J. Li, K. Xie, Y. Lai, Z. Zhang, F. Li, X. Hao, X. Chen, Y. Liu, *J. Power Sources* **2010**, *195*, 5344–5350; d) Z. Zhang, X. Chen, F. Li, Y. Lai, J. Li, P. Liu, X. Wang, *J. Power Sources* **2010**, *195*, 7397–7402; e) F. Wu, J. Qian, R. Chen, J. Lu, L. Li, H. Wu, J. Chen, T. Zhao, Y. Ye, K. Amine, *ACS Appl. Mater. Interfaces* **2014**, *6*, 15542–15549.
[14] P. C. Howlett, D. R. MacFarlane, A. F. Hollenkamp, *Electrochem. Solid-State Lett.* **2004**, *7*, A97–A101.
[15] B. Philippe, R. Dedryvere, M. Gorgoi, H. Rensmo, D. Gonbeau, K. Edstrom, *J. Am. Chem. Soc.* **2013**, *135*, 9829–9842.
[16] Q. C. Liu, J. Xu, S. Yuan, Z. Chang, D. Xu, X. Zhan, *Adv. Mater.* **2015**, *27*, 5241–5247.
[17] D. Aurbach, *J. Power Sources* **2000**, *89*, 206–218.
[18] L. Wang, X. He, J. Li, M. Chen, J. Gao, C. Jiang, *Electrochim. Acta* **2012**, *72*, 114–119.
[19] S. S. Zhang, *Electrochem. Commun.* **2006**, *8*, 1423–1428.
[20] J. Wang, Z. Yao, C. W. Monroe, J. Yang, Y. Nuli, *Adv. Funct. Mater.* **2013**, *23*, 1194–1201.

Received: June 19, 2016
Published online: July 27, 2016

